

^1H NMR Investigation of Thermally Triggered Insulin Release from Poly(*N*-isopropylacrylamide) Microgels

Christine M. Nolan, Leslie T. Gelbaum, and L. Andrew Lyon*

*School of Chemistry and Biochemistry and Petit Institute for Bioengineering and Bioscience,
Georgia Institute of Technology, Atlanta, Georgia 30332-0400*

Received July 22, 2006; Revised Manuscript Received August 15, 2006

We describe investigations of insulin release from thermoresponsive microgels using variable temperature ^1H NMR. Microgel particles composed of poly(*N*-isopropylacrylamide) were loaded with the peptide via a swelling technique, and this method was compared to simple equilibrium partitioning. Variable temperature ^1H NMR studies suggest that the swelling loading method results in enhanced entrapment of the peptide versus equilibrium partitioning. A centrifugation-loading assay supports this finding. Pseudo-temperature jump ^1H NMR measurements suggest that the insulin release rate is partially decoupled from microgel collapse. These types of direct release investigations could prove to be useful methods in the future design of controlled macromolecule drug delivery devices.

Introduction

Within the past decade, the fabrication of stimuli-responsive hydrogels^{1,2} has been increasingly investigated for controlled drug release applications.^{3–8} Poly(*N*-isopropylacrylamide) (pNIPAm)⁹ has been one of the most heavily explored polymers for the fabrication of thermosensitive hydrogels. These gels undergo a reversible volume phase transition at a characteristic volume phase transition temperature (VPTT) of 31 °C, where the network goes from a highly solvent swollen state to a collapsed dehydrated network. Above this VPTT, the hydrogel collapses upon itself expelling water in an entropically driven fashion. This reversible deswelling event has been used as a means to control uptake and release of various model drugs.

In recent years, a significant amount of work has focused on using responsive gels as carriers for peptide delivery both in monolithic, bulk gels^{10–13} and discrete microgel systems.^{14–17} Among these numerous studies on protein delivery, much work has focused on macroscopic hydrogel insulin release systems.^{18–20} For example, Peppas et al. employed pH sensitive hydrogels for insulin delivery with the main goal being oral release.^{21–26} Self-regulating insulin delivery systems that utilize pH responsiveness as a means to respond to increases in free glucose concentration have also been investigated.^{27,28} Superporous hydrogel networks²⁹ and biodegradable hydrogel networks are yet another area of insulin release devices that have been researched.^{30–32} Insulin is a therapeutic agent that is known to be endogenously released in a pulsatile manner^{33–37} and hence, oscillatory insulin release from hydrogel systems has also been explored.³⁸ Work done by Siegel et al. has proposed a general strategy for pulsatile drug release³⁹ and these studies have been extended to self-regulated hormone release systems.^{40,41} The use of discrete microgel particles for controlled insulin delivery has also been described.^{42–45}

Our group has previously reported on the thermally modulated insulin release from layer-by-layer (LbL) assembled pNIPAm-co-acrylic acid (pNIPAm-AAc) microgel thin films.⁴⁶ In that

work, insulin was loaded by increasing the pH above the AAc pK_a , thereby driving a microgel swelling transition. It was hypothesized that this swelling drove insulin incorporation. The thin films were then shown to release insulin in a temperature dependent fashion due to the thermally induced deswelling of pNIPAm. A more dramatic swelling response that can be used for loading is that which occurs when the dried polymer is allowed to rehydrate in a solution of the molecule to be loaded. This “breathing-in” technique has been used previously to entrap solutes in hydrogel networks. In this paper, we take advantage of this spongelike nature of the microgels, thereby allowing solute molecules to partition into the porous network. This technique was directly compared to a simple equilibrium partitioning strategy where an already swollen microgel solution was mixed with an insulin solution. To directly monitor the thermally triggered insulin release into solution, we utilized ^1H NMR as a probe, considering the fact that similar release events have been previously studied in such a manner.⁴⁷ These studies suggest that this method could be broadly applied to the monitoring of solute release from dispersed microgels.

Experimental Section

Materials. All chemicals were obtained from Sigma Aldrich unless otherwise stated. The monomer *N*-isopropylacrylamide (NIPAm) was recrystallized from hexanes (J. T. Baker) prior to use. The cross-linker *N,N'*-methylenebis(acrylamide) (BIS), sodium dodecyl sulfate (SDS), ammonium persulfate (APS), deuterium oxide (D_2O), deuterated hydrochloric acid (DCl), sodium deuterioxide (NaOD), deuterated acetone, and insulin (from bovine pancreas) were used as received. For purification purposes, 0.2 μm nylon membrane disks and a Spectra/Por 10 000 MWCO dialysis membrane were purchased from VWR. Water used in all experiments was distilled and then purified using a Barnstead E-Pure system operating at a resistance of 18 M Ω . A 0.2 μm filter was incorporated into this system to remove particulate matter.

Particle Synthesis. Microgels cross-linked with 2 mol % BIS were synthesized by precipitation polymerization via a method slightly modified from that previously described.⁴⁸ The total monomer concentration was 100 mM in all reactions. The surfactant was SDS, and APS was used as the free radical initiator. The NIPAm monomer, cross-linker, and surfactant (0.01 g) were dissolved in 200 mL of distilled,

* To whom correspondence should be addressed. E-mail: LL62@mail.gatech.edu.

deionized water, filtered through a 0.2 μm nylon membrane filter to remove any particulate matter, and then continuously stirred in a three-neck, 250 mL round-bottom flask. This solution was heated to 70 $^{\circ}\text{C}$ while being purged with N_2 gas. Approximately 1 h later, the temperature of the solution was stable at 70 $^{\circ}\text{C}$. After 15 min, the reaction was initiated by adding a solution of APS (1 mM final concentration). The solution turned turbid within 10 min, indicating successful initiation. The reaction proceeded for 6 h under a constant stream of N_2 . Following synthesis, the microgels were filtered using a P2 Whatman filter paper and then dialyzed (using 10 000 MWCO) for 2 weeks against distilled, deionized water with a daily exchange of the water.

Photon Correlation Spectroscopy (PCS). Hydrodynamic radii and light scattering intensities were obtained by PCS (Protein Solutions, Inc.). Prior to analysis, the purified microgels were diluted in filtered, distilled, deionized water (using 0.2 μm filters) until a count rate of 350 kCt/s was obtained. The suspensions were then held at each temperature for 15 min to achieve thermal equilibration before measurements were taken. Longer equilibration times did not result in variations of particle radius, polydispersity, or light scattering intensity. The data points presented here are an average of 5 measurements with a 60 s acquisition time. Hydrodynamic radii were calculated from the measured diffusion coefficients using the Stokes–Einstein equation. All correlogram analyses were performed with manufacturer-supplied software (Dynamics v.5.25.44, Protein Solutions, Inc.).

Impregnation of Microgels with Insulin. Two insulin loading strategies were compared. The first was to swell lyophilized microgels in a concentrated solution of insulin for 24 h. Insulin is difficult to dissolve from the powdered form in neutral pH media but is quite soluble under acidic conditions.²⁹ Thus, the insulin was first dissolved in DCI to prepare the stock solution,²⁹ and then the pH was increased by addition of NaOD until a pH of 7.4 was achieved. A final insulin concentration of 31 mg/mL was achieved. A known volume of diluted stock solution was then added to a known mass of lyophilized microgels (15.2 mg), and the particles were allowed to swell in this solution for 24 h. The overall concentration of insulin in the final solution was 15 mg/mL.

For the physical mixture, the same mass of lyophilized microgels (15.2 mg) was dissolved in D_2O and allowed to swell overnight on a shaker table. The already swollen dispersion of microgels was then physically mixed with a known volume of diluted insulin stock solution to yield the same overall concentration of insulin (15 mg/mL). This mixture was allowed to equilibrate overnight on a shaker table. Note that the “free” insulin was *not* removed by centrifugation prior to the NMR measurements. This allowed us to analyze the relative strengths of the insulin and polymer resonances between the two loading methods for samples with identical concentrations of each component. As discussed below, these differences in peak area can presumably be related to the relative degrees of mobility for each component.

^1H NMR. A Bruker Avance DRX 500 MHz NMR spectrometer was used for the insulin release investigations. Lyophilized microgels (1.0 mg) and insulin (8.0 mg) were separately dissolved in 1 mL of D_2O and the spectra of each were recorded at 25 $^{\circ}\text{C}$. Spectra of insulin loaded microgels were also recorded at 25 $^{\circ}\text{C}$. For the variable temperature studies, spectra of loaded microgels were taken at 25, 28, 31, 34, and 37 $^{\circ}\text{C}$. For these studies, before taking measurements, the samples were thermally equilibrated for 15 min at each temperature. No changes in the signal intensities were observed if the equilibration time was prolonged. For the temperature jump study, the NMR spectrometer probe was set at either 34, 37, or 40 $^{\circ}\text{C}$ and a cool (25 $^{\circ}\text{C}$) insulin impregnated sample was inserted into the spectrometer. Spectra were immediately recorded every 7.5 s; a total of 39 spectra were recorded. For all variable temperature studies, a deuterated acetone external standard was used, where the acetone solution was inserted into a microcapillary, which was then sealed. This standard was then directly inserted into the center of the NMR tube containing the insulin-loaded microgel solutions. The integrated ratios of the main pNIPAm

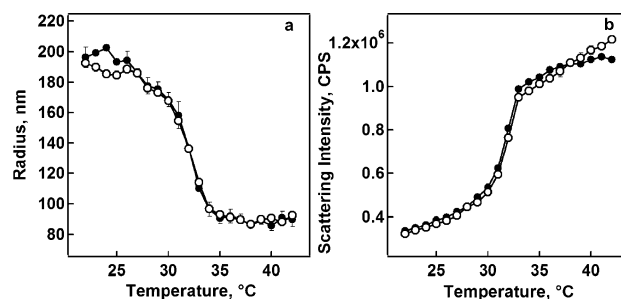


Figure 1. (a) Volume phase transition curves for pNIPAm microgels (filled circles) and those particles loaded with insulin via swelling of dried particles (open circles); (b) corresponding light scattering profiles for pNIPAm microgels (filled circles) and those particles loaded with insulin via swelling of dried particles (open circles).

peak at 1.1 ppm and the insulin peaks from 6.6 to 7.4 ppm were normalized with respect to the residual protons in the deuterated acetone standard. The main pNIPAm peak was chosen for integration due to its strong signal, whereas the insulin peaks from 6.6 to 7.4 ppm were chosen due to the lack of spectral overlap with polymer resonances.

Centrifugation Loading Assay. Following ^1H NMR analyses, both types of insulin loaded microgels (swollen and mixed) were transferred to 2 mL Eppendorf tubes and centrifuged at 16 000g rcf at 26 $^{\circ}\text{C}$ for 20 min. Following this, 250 μL of supernatant was extracted from each sample and then diluted with 4 mL of 20 mM PBS. The absorption spectra of these samples were analyzed via UV/vis spectroscopy along with a control sample containing the same overall concentration of insulin as the loaded samples without any microgels present. The percent of insulin loaded was then calculated against the control sample.

Results and Discussion

As described above, 2 mol % BIS cross-linked pNIPAm microgels were chosen for these insulin loading and release investigations. We have previously reported results on insulin-impregnated microgels that contained pH sensitive acrylic acid groups.⁴⁶ This pH responsivity allowed the microgels to swell under neutral pH conditions and was hypothesized to be the main driving force allowing for insulin partitioning into the particles. In this current study, we wanted to remove any contributions from pH responsivity of the microgel in order to simplify the analysis. Hence, microgels without acrylic acid comonomer were investigated. Two loading strategies were compared. The first was to swell lyophilized microgels in a concentrated solution of insulin for 24 h. The second method entailed a simple equilibrium partitioning technique whereby an already swollen microgel solution was physically mixed with an insulin solution. Both strategies utilized the same mass of dried microgels to start with and used the same overall concentration of insulin so they could be directly compared to one another.

To probe the effect that insulin impregnation has on the phase transition behavior of 2 mol % BIS cross-linked microgels, the hydrodynamic radius was measured as a function of temperature for both insulin loaded microgels (via the swelling technique) and unloaded microgels using PCS. Figure 1a shows the volume phase transition behavior of these two samples, where the open circles represent the loaded sample and the filled circles represent the microgels alone. At low temperatures, both sets of particles display approximately the same average hydrodynamic radius of 190 nm. The loaded and unloaded microgel networks both undergo a sharp volume phase transition at approximately 32 $^{\circ}\text{C}$ after which they deswell to a minimum hydrodynamic radius of approximately 90 nm. The VPTT for

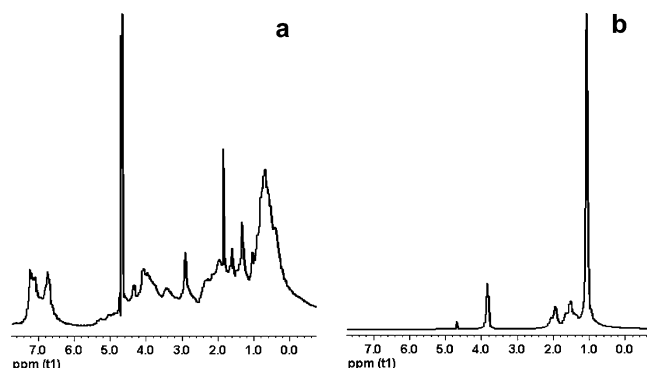


Figure 2. ¹H NMR spectra of (a) insulin (pH adjusted to 7.4) and (b) pNIPAm microgels in D₂O at 25 °C.

both sets of particles corresponds well with the VPTT of typical pNIPAm microgels.⁴⁹ Figure 1b shows the corresponding light scattering profiles of the same samples. Both sets of particles display very little scattered light intensity at temperatures below the VPTT. This is because these porous microgel networks are highly solvent swollen and are therefore nearly index matched to their environment (water). When the microgels collapse into dense globules at temperatures above the VPTT, the microgels display a higher scattering cross section, and a concomitant increase in scattered light intensity is observed from the suspensions above the VPTT. These results suggest that impregnation of the microgels with insulin does not perturb the deswelling thermodynamics or swelling capacities to a significant extent.

To design direct release experiments, ¹H NMR spectra of insulin in D₂O (pH 7.4) and 2 mol % BIS cross-linked microgels were first taken at 25 °C to determine if spectral resolution could be achieved. The spectrum of insulin is shown in Figure 2a; this spectrum is in agreement with literature reports of its spectrum acquired at neutral pH.⁵⁰ Figure 2b shows the spectra obtained for the 2 mol % BIS cross-linked microgels; the proton assignments for the pNIPAm polymer also suitably correspond to its chemical structure.^{33,34} The peak at 1.1 ppm can be attributed to the methyl protons of the *N*-isopropyl group. The resonance for the methylene proton of the isopropyl group is observed at 3.8 to 4.0 ppm, whereas the resonances from 1.2 to 2.2 ppm are attributed to the protons on the polymer backbone. In all ¹H NMR spectra, the peak at approximately 4.7 ppm is the suppressed solvent water peak. Although there is some spectral overlap within the region of 0.0 to 4.0 ppm, the most intense peak from the pNIPAm polymer at approximately 1.0 ppm is somewhat spectrally distinct. Furthermore, there is no spectral overlap for the downshifted insulin peaks from 6.6 to 7.4 ppm. It is these two peak signals that will be interrogated as a function of temperature to try and probe direct insulin expulsion from impregnated particles.

To probe feasibility of detecting an increase in insulin signal due to expulsion from the microgels using NMR, spectra of insulin-loaded 2 mol % BIS cross-linked microgel samples were recorded at temperatures both below and above the VPTT of the particles. These results are shown in Figure 3. Panels a and b show the spectra for insulin-loaded microgels prepared via the breathing-in technique at 25 and 37 °C, respectively. In these spectra, as mentioned in the Experimental Section, the residual proton signal from a deuterated acetone external standard was used for normalization and its resonance is observed at approximately 2.9 ppm. This resonance is somewhat shifted from what is expected since the water peak at 4.7 ppm was used as a reference. The spectra shown in panels c and d correspond to

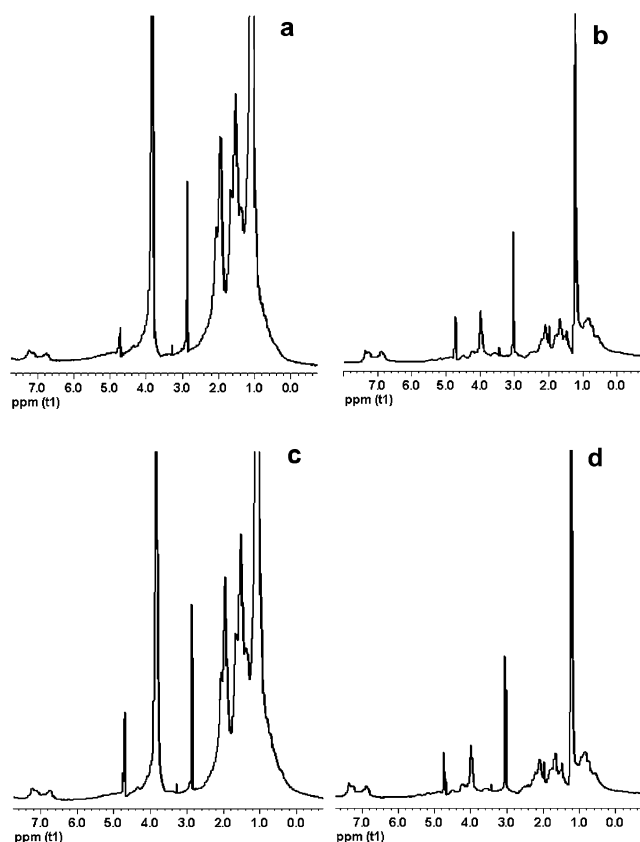


Figure 3. ¹H NMR spectra of insulin-loaded pNIPAm microgels at temperatures below and above the volume phase transition temperature (overall pH 7.4). (a) Spectrum taken at 25 °C of microgels loaded with insulin via the breathing-in technique, (b) spectrum taken at 37 °C of microgels loaded with insulin via the breathing-in technique, (c) spectrum taken at 25 °C of microgels loaded via equilibrium partitioning at 25 °C, and (d) spectrum taken at 37 °C of microgels loaded via equilibrium partitioning at 25 °C.

the sample loaded via simple equilibrium partitioning at temperatures below and above the VPTT, respectively. For both sets of particles, at 25 °C the pNIPAm resonances dominate the spectra and only relatively small insulin peaks are observable in the aromatic region of the spectrum. Under these conditions, it is presumed that most of the insulin is impregnated within the microgel interior. Hence, the signal due to insulin is diminished due to lack of free rotation in the microgel network. When the temperature is raised above the VPTT to 37 °C, the particles deswell and release insulin into surrounding solution resulting in an increase in the insulin signal with respect to the acetone standard. It is clearly evident that for both types of insulin-loaded microgels a relative increase in the ratios of insulin/acetone occurs upon elevation in temperature from 25 to 37 °C, whereas a concomitant decrease in the pNIPAm/acetone ratios is observed upon particle collapse. At elevated temperatures, the pNIPAm resonances become significantly depressed due to the fact that as the microgel collapses it becomes denser and more solidlike.^{51–53} These results suggest that microgel deswelling results in osmotically driven insulin expulsion from the network as the free volume in the microgel interior decreases.

To probe this release event in more detail, ¹H NMR spectra were obtained every three degrees from 25 to 37 °C. The results for these experiments are shown in Figure 4. Figure 4a shows the normalized pNIPAm/acetone peak ratios as a function of temperature for the microgels that were loaded by the breathing-in technique (open circles) and by equilibrium partitioning (open

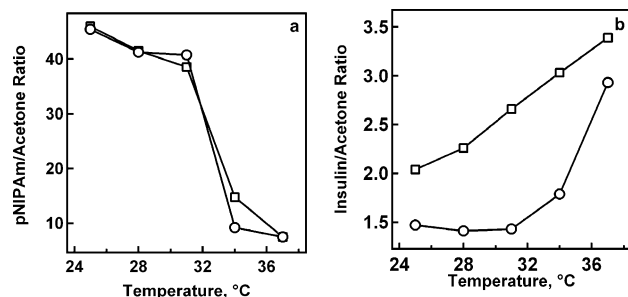


Figure 4. Plots of the normalized ratios of (a) pNIPAm/acetone and (b) insulin/acetone as a function of temperature. Open circles represent microgels loaded via the breathing-in technique; open squares represent microgels loaded via equilibrium partitioning.

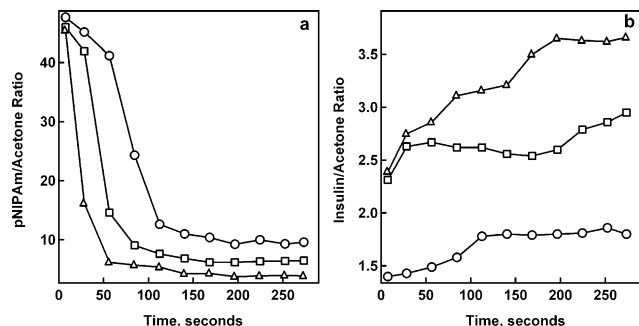


Figure 5. Plots of microgel deswelling (a) and insulin release (b) for an insulin loaded microgel sample (via swelling) subjected to a temperature jump from 25 to 34 (open circles), 37 (open squares), or 40 °C (open upward triangles).

squares). This plot illustrates that the temperature at which both sets of loaded microgels deswell corresponds well with the well-known phase transition temperature of 32 °C.⁴⁹ These profiles also correlate well with the VPTT curves obtained for the loaded and unloaded samples shown in Figure 1a. Figure 4b shows the peak ratios of insulin/acetone as a function of temperature for both insulin-loaded samples. A distinct difference in the release profiles is observed here where the normalized insulin signal for the physical mixture (open squares) is consistently higher than that for the swollen sample (open circles) at all temperatures. This suggests that the breathing-in technique results in enhanced entrapment of the peptide versus simple mixing, and hence, not as much insulin is free in solution to be detected. The slopes of the two profiles are also distinctly different. The sample loaded by the breathing-in technique (open circles) does not display a significant increase in normalized insulin signal until 34 and 37 °C, whereas the sample loaded via equilibrium partitioning shows a steady increase over the entire temperature range. We hypothesize that the microgels loaded by mixing perhaps contain a significant amount of surface-adsorbed insulin, which may result in a temperature dependent release that is less coupled to the phase transition of the hydrogel itself. The sample impregnated via the breathing-in technique, however, effectively entraps insulin in the particle interior, and it is not until the microgel partially or fully deswells that entrapped species are expelled into solution.

The early stages of insulin release were studied using a ¹H NMR temperature jump investigation. In this study, an insulin-impregnated sample (via breathing in) held at 25 °C was quickly inserted into the NMR spectrometer that was equilibrated at 34, 37, or 40 °C. Following insertion, spectra were collected every 7.5 s. The results of this experiment are shown in Figure 5. Figure 5a shows the profiles for microgel collapse as a function of time and temperature. It is clear that differences in microgel deswelling rates occur depending upon the temperature

Table 1. Insulin Loading Results for 2 mol % BIS Cross-Linked Microgels and ¹H NMR Normalized Ratios of pNIPAm and Insulin.

insulin loaded microgel sample	obtained via UV/vis % loaded insulin	obtained via ¹ H NMR at 25 °C	
		pNIPAm/acetone ratio	insulin/acetone ratio
via swelling	40	45	1.5
via equilibrium partitioning	23	46	2.0

differential used, with the 40 °C temperature jump resulting in fastest equilibration. Note that all “rates” shown here are convoluted with the thermal equilibration of the NMR tube itself, and therefore, what is really being measured is the rate of thermal equilibration with the probe. Thermal equilibration of course will be dependent on the temperature difference between the sample and the probe. The magnitudes of deswelling are also distinctly different depending upon the applied temperature differential. Figure 5b illustrates the corresponding insulin release profiles for each temperature jump. The 34 °C jump shows that some insulin release occurs within the first 110 s, and then this profile plateaus. This is most likely due to the fact that the microgels at this temperature are not fully deswollen and some of the insulin remains embedded within the microgel interior after an initial burst of release. The 37 °C temperature jump shows a somewhat different profile. Some release occurs within the first 60 s corresponding to the time course of the deswelling event at this temperature. This release, however, levels off after this up until approximately 220 s where slightly more insulin expulsion occurs. The 40 °C temperature jump experiment shows higher insulin/acetone ratios at all times, thus indicating a significant amount of insulin gets immediately released once the sample is inserted. This release profile gradually increases with time suggesting gradual insulin partitioning out of the network.

To ascertain the actual loading efficiency of each strategy, a centrifugation loading assay was performed following NMR analyses. The loaded samples were allowed to reswell at 4 °C overnight and were then centrifuged and analyzed as described in the Experimental Section. The results for these experiments are shown in Table 1 along with a summary of the normalized pNIPAm and insulin ratios obtained in the ¹H NMR release studies. Note that these values represent the results obtained from a single sample set. Replicates of these experiments were performed on a lower field strength instrument, and were therefore not rigorously comparable from a statistical analysis point of view. However, we estimate from those measurements that the loading method is reproducible with a precision of approximately ±10%. These results confirm the previous conclusions that the breathing-in technique does result in enhanced loading of insulin. The fact that the normalized insulin signal at 25 °C is higher for the physical mixture versus the sample loaded by swelling suggests effective peptide entrapment with the breathing-in technique.

The results presented above clearly indicate that the two methods of insulin loading produce very different final products. For the physical mixture, it is apparently the case that the peptide does not diffuse into the microgel interior to a very great extent and may simply adsorb to the periphery of the microgel. This conclusion is based on our observations of an almost 2-fold lower loading efficiency and a strong decoupling of the insulin release from the volume phase transition of the microgels. If the insulin were loaded and/or strongly associated with the network polymer, we would expect the large change of the

microgel's volume at the phase transition to result in insulin expulsion, as we have observed previously for hydrogel thin films loaded with insulin^{46,54} and doxorubicin.⁵⁵ We hypothesize that the interactions between the microgel and insulin under these loading conditions are primarily due to hydrogen bonding to the amide groups on the polymer side chains. Penetration of the peptide deeper within the microgel may be sterically prohibitive due to the torturous path through the hydrogel network. Although we have not undertaken rigorous studies of longer equilibration times in order to investigate whether penetration occurs on a longer time scale, it is clear that any such penetration does not occur to an appreciable extent on the time scale of 10–20 h (the equilibration times used in these studies).

Conversely, the particles loaded by “breathing-in” display a higher degree of loading and a release of insulin that is very strongly coupled to particle deswelling. In this case, it is likely that the insulin is adsorbed within the microgel both by hydrogen bonding as well as simple physical entrapment. The hypothesis in this case is that insulin incorporation is largely driven by the rapid influx of water into the polymer network, which would result in a similarly rapid transport of solutes. Once inside the network, the insulin could associate with the polymer or simply reside in pores in the network. The ability of the peptide to passively diffuse out of the polymer would be opposed by the sterically (entropically) disfavored motion through the torturous hydrogel network. This type of entrapment has been demonstrated previously for nano- and microstructured gels in a set of brilliant experiments reported by Liu and Asher.⁵⁶

Conclusions

A macromolecular therapeutic agent, insulin, was rapidly and effectively impregnated into thermoresponsive pNIPAm microgels via a breathing-in technique that proved to be superior over simple equilibrium partitioning. Thermally induced release was directly monitored using ¹H NMR, which suggested that the swelling strategy results in efficient entrapment of the peptide. A ¹H NMR temperature jump study was also performed. This study suggests that the rate at which insulin is released from the loaded network is partially decoupled from its collapse and that multiple stages of release exist as a function of temperature. These types of direct release experiments could prove as useful templates in the future design of controlled macromolecule release devices utilizing functionally modified thermoresponsive particles.

Acknowledgment. L.A.L. acknowledges support from the ACS-PRF and partial support through an NSF-CAREER award (CHE-9984012).

References and Notes

- Tanaka, T. *Phys. Rev. Lett.* **1978**, *40*, 820–823.
- Tanaka, T.; Sato, E.; Hirokawa, Y.; Hirotsu, S.; Peetermans, J. *Phys. Rev. Lett.* **1985**, *55*, 2455–2458.
- Peppas, N. A.; Leobandung, W. *J. Biomater. Sci., Polym. Ed.* **2004**, *15*, 125–144.
- Siegel, R. A.; Ziaie, B. *Adv. Drug Delivery Rev.* **2004**, *56*, 121–123.
- Kikuchi, A.; Okano, T. *Adv. Drug Delivery Rev.* **2002**, *54*, 53–77.
- Hoffman, A. S. *Adv. Drug Delivery Rev.* **2002**, *54*, 3–12.
- Qiu, Y.; Park, K. *Adv. Drug Delivery Rev.* **2001**, *53*, 321–339.
- Kopecek, J.; Kopeckova, P.; Minko, T.; Lu, Z. R.; Peterson, C. M. *J. Controlled Release* **2001**, *74*, 147–153.
- Heskins, M.; Guillet, J. E. *J. Macromol. Sci. Chem.* **1968**, *A2*, 1441–1455.
- Jong, S. J. d.; van Eerdenbrugh, B.; van Nostrum, C. F.; den Bosch, J. J. K.-v.; Hennink, W. E. *J. Controlled Release* **2001**, *71*, 261–275.
- Gehrke, S. H.; Uhden, L. H.; McBride, J. F. *J. Controlled Release* **1998**, *55*, 21–33.
- Edelman, E. R.; Brown, L.; Langer, R. *J. Pharm. Sci.* **1996**, *85*, 1271–1275.
- Carino, G. P.; Jacob, J. S.; Mathiowitz, E. *J. Controlled Release* **2000**, *65*, 261–269.
- Mellott, M. B.; Searcy, K.; Pishko, M. V. *Biomaterials* **2001**, *22*, 929–941.
- Murthy, N.; Xu, M.; Schuck, S.; Kunisawa, J.; Shastri, N.; Frechet, J. M. J. *Proc. Natl. Acad. Sci.* **2003**, *100*, 4995–5000.
- Wang, N.; Wu, X. S.; Li, J. K. *Pharm. Res.* **1999**, *16*, 1430–1435.
- Slager, J.; Domb, A. J. *Biomaterials* **2002**, *23*, 4389–4396.
- Yu, H.; Grainger, D. W. *J. Controlled Release* **1995**, *34*, 117–127.
- Park, T. G. *Biomaterials* **1999**, *20*, 517–521.
- Kagatani, S.; Shinoda, T.; Konno, Y.; Fukui, M.; Ohmura, T.; Osada, Y. *J. Pharm. Sci.* **1997**, *86*, 1273–1277.
- Morishita, M.; Lowman, A. M.; Takayama, K.; Nagai, T.; Peppas, N. A. *J. Controlled Release* **2002**, *81*, 25–32.
- Torres-Lugo, M.; Garcia, M.; Record, R.; Peppas, N. A. *J. Controlled Release* **2002**, *80*, 197–205.
- Robinson, D. N.; Peppas, N. A. *Macromolecules* **2002**, *35*, 3668–3674.
- Kim, B.; Peppas, N. A. *Int. J. Pharm.* **2003**, *266*, 29–37.
- Torres-Lugo, M.; Garcia, M.; Record, R.; Peppas, N. A. *Biotechnol. Prog.* **2002**, *18*, 612–616.
- Lowman, A. M.; Morishita, M.; Kajita, M.; Nagai, T.; Peppas, N. A. *J. Pharm. Sci.* **1999**, *88*, 933–937.
- Traitel, T.; Cohen, Y.; Kost, J. *Biomaterials* **2000**, *21*, 1679–1687.
- Kim, J. J.; Park, K. *J. Controlled Release* **2001**, *77*, 39–47.
- Dorkoosh, F. A.; Verhoef, J. C.; Ambagts, M. H. C.; Rafiee-Tehrani, M.; Borchard, G.; Junginger, H. E. *Eur. J. Pharm. Sci.* **2002**, *15*, 433–439.
- Moriyama, K.; Yui, N. *J. Controlled Release* **1996**, *42*, 237–248.
- Zhang, Y.; Chu, C.-C. *J. Biomater. Appl.* **2002**, *16*, 305–325.
- Watnasirichaikul, S.; Davies, N. M.; Rades, T.; Tucker, I. G. *Pharm. Res.* **2000**, *17*, 684–689.
- Chou, H. F.; Ipp, E. *Diabetes* **1990**, *39*, 112–117.
- Goodner, C. J.; Walike, B. C.; Koerker, D. J.; Ensink, J. W.; Brown, A. C.; Chideckel, E. W.; Palmer, J.; Kalnasy, L. *Science* **1977**, *195*, 177–179.
- Hansen, B. C.; Jen, K. C.; Belbez, P. S.; Wolfe, R. A. *J. Clin. Endocrinol. Metab.* **1982**, *54*, 785–792.
- Lang, D. A.; Matthews, D. R.; Burnett, M.; Turner, R. C. *Diabetes* **1981**, *30*, 435–439.
- Porksen, N.; Munn, S.; Steers, J.; Vore, S.; Veldhuis, J.; Butler, P. *Am. J. Physiol.* **1995**, *269*, E478–E488.
- Moriyama, K.; Tooru, O.; Nobuhiko, Y. *J. Biomater. Sci., Polym. Ed.* **1999**, *10*, 1251–1264.
- Siegel, R. A.; Colin, G. P. *J. Controlled Release* **1995**, *33*, 173–188.
- Misra, G. P.; Siegel, R. A. *J. Controlled Release* **2002**, *81*, 1–6.
- Siegel, R. A.; Gu, Y.; Bladi, A.; Ziaie, B. *Macromol. Symp.* **2004**, *207*, 249–256.
- Kwong, A. K.; Chou, S.; Sefton, M. V. *J. Controlled Release* **1986**, *4*, 47–62.
- Soriano, I.; Evora, C.; Llabres, M. *Int. J. Pharm.* **1996**, *142*, 135–142.
- Leobandung, W.; Ichikawa, H.; Fukumori, Y.; Peppas, N. A. *J. Controlled Release* **2002**, *80*, 357–363.
- Damge, C.; Vranckx, H.; Balschmidt, P.; Couvreur, P. *J. Pharm. Sci.* **1997**, *86*, 1403–1409.
- Nolan, C. M.; Serpe, M. J.; Lyon, L. A. *Biomacromolecules* **2004**, *5*, 1940–1946.
- Sass, H.-J.; Musco, G.; Stahl, S. J.; Wingfield, P. T.; Grzesiek, S. *J. Biomol. NMR* **2000**, *18*, 303–309.
- Jones, C. D.; Lyon, L. A. *Macromolecules* **2000**, *33*, 8301–8306.
- Pelton, R. H. *Adv. Colloid. Interface Sci.* **2000**, *85*, 1–33.
- Williamson, K. L.; Williams, R. J. P. *Biochemistry* **1979**, *18*, 5966–5972.
- Gan, D.; Lyon, L. A. *Macromolecules* **2002**, *35*, 9634–9639.
- Schoenhoff, M.; Schwarz, B.; Larsson, A.; Kuckling, D. *Prog. Colloid Polym. Sci.* **2002**, *121*, 80–87.
- Schoenhoff, M.; Larsson, A.; Welzel, P. B.; Kuckling, D. *J. Phys. Chem. B* **2002**, *106*, 7800–7808.
- Nolan, C. M.; Serpe, M. J.; Lyon, L. A. *Macromol. Symp.* **2005**, *227*, 285–294.
- Serpe, M. J.; Yarmey, K. A.; Nolan, C. M.; Lyon, L. A. *Biomacromolecules* **2004**, *6*, 408–413.
- Liu, L.; Li, P. S.; Asher, S. A. *Nature* **1999**, *397*, 141–144.